

Article

# Similarity Classes in the Eight-Tetrahedron Longest-Edge Partition of a Regular Tetrahedron

Miguel A. Padrón <sup>†</sup> , Ángel Plaza <sup>†</sup>  and José Pablo Suárez <sup>\*,†</sup> 

IUMA Information and Communications System, University of Las Palmas de Gran Canaria, 35017 Las Palmas de Gran Canaria, Spain; miguel.padrón@ulpgc.es (M.A.P.); angel.plaza@ulpgc.es (Á.P.)

\* Correspondence: josepablo.suarez@ulpgc.es

<sup>†</sup> These authors contributed equally to this work.

**Abstract:** A tetrahedron is called regular if its six edges are of equal length. It is clear that, for an initial regular tetrahedron  $R_0$ , the iterative eight-tetrahedron longest-edge partition (8T-LE) of  $R_0$  produces an infinity sequence of tetrahedral meshes,  $\tau^0 = \{R_0\}$ ,  $\tau^1 = \{R_i^1\}$ ,  $\tau^2 = \{R_i^2\}$ , ...,  $\tau^n = \{R_i^n\}$ , ... In this paper, it is proven that, in the iterative process just mentioned, only two distinct similarity classes are generated. Therefore, the stability and the non-degeneracy of the generated meshes, as well as the minimum and maximum angle condition straightforwardly follow. Additionally, for a standard-shape tetrahedron quality measure ( $\eta$ ) and any tetrahedron  $R_i^n \in \tau^n$ ,  $n > 0$ , then  $\eta(R_i^n) \geq \frac{2}{3}\eta(R_0)$ . The non-degeneracy constant is  $c = \frac{2}{3}$  in the case of the iterative 8T-LE partition of a regular tetrahedron.

**Keywords:** regular tetrahedron; similarity classes; 8T-LE partition; normalized sextuple; longest-edge bisection; strong stability; refinement; meshes

**MSC:** 65L50; 74S05; 78M25



**Citation:** Padrón, M.A.; Plaza, Á.; Suárez, J.P. Similarity Classes in the Eight-Tetrahedron Longest-Edge Partition of a Regular Tetrahedron. *Mathematics* **2023**, *11*, 4456. <https://doi.org/10.3390/math11214456>

Academic Editor: Rade Vignjevic

Received: 8 September 2023

Revised: 15 October 2023

Accepted: 18 October 2023

Published: 27 October 2023



**Copyright:** © 2023 by the authors. Licensee MDPI, Basel, Switzerland. This article is an open access article distributed under the terms and conditions of the Creative Commons Attribution (CC BY) license (<https://creativecommons.org/licenses/by/4.0/>).

## 1. Introduction

The development of the automatic adaptive finite element analysis procedure has received much attention, since such programs allow us to obtain an efficient approximate solution of partial differential equations, which can be found in a wide variety of engineering problems, such as fluid mechanics problems, temperature distribution, structural analysis, etc. The mesh generation, adaptivity, non-degeneracy, and local refinement of the mesh play a very significant role when a prescribed accuracy has to be achieved by controlling the discretization error subdividing the elements of the mesh [1,2]. In three dimensions, the problem size and, hence, the computational cost can grow very quickly under the refinement process.

In general, mesh-refinement strategies for tetrahedral meshes can be separated into two main groups: octasection [3–5] and bisection methods [6–11]. Methods based on octasections simultaneously subdivide any given tetrahedron into eight subtetrahedra of equal volume.

After cutting off four subtetrahedra at the corners, which are congruent to the father, the remaining octahedron is subdivided by choosing one of the three possible interior diagonals. The election of this interior diagonal has to be performed carefully to satisfy the stability condition [3,5]. On the other hand, methods based on the bisection can also subdivide a tetrahedron into eight, but the first step is to subdivide the tetrahedron into two subtetrahedra by adding a new point on some particular edge and connecting it to the vertices opposite that edge. When the chosen edge is the longest one of the tetrahedron, the method is called the longest-edge bisection. The accuracy of the numerical solution associated with these methods depends strongly on the shape quality of the elements [12,13].

Bisection-based tetrahedral partitions have been studied thoroughly in recent years [6–10,14,15]. A comparative study of some of them can be found in [16]. Tetrahedral bisections are the natural extension to 3D of their counterparts in 2D [6–11].

The 8T-LE partition is also based on the bisection, and it is the natural extension to 3D of its 2D counterpart introduced and studied by Rivara [17], the four-triangle longest-edge partition (4T-LE). The self-improvement property, non-degeneracy, and locality of the refinement are very convenient properties of this partition in its application for solving problems with the finite element method.

A problem that remains open is to know if the repeated 8T-LE partition of tetrahedra generates a finite number of new shape classes or not; although, the numerical examples carried out in [18] suggest a good behavior for this partition.

Recently, the regular tetrahedron has received much attention in areas such as global optimization for mixture design by using the so-called branch-and-bound methods, where the regular  $n$ -simplex is bisected [19,20]. Additionally, this tetrahedron can be found in the triangulation of the 3D cube into five tetrahedra, and the building of the nearly equilateral tetrahedra carried out by Adler in 1983 [21] was also based on the regular tetrahedron. It should be noted that the regular tetrahedron poses a critical case in the bisection methods, as all edges have equal lengths. The difficulty arises as the refinement edge cannot be uniquely determined, especially when the longest edge is first bisected. Then, a combinatorial situation appears when computing similarity classes during refinement. Irregular tetrahedra also hold a different complex situation when commuting similarity classes, in part due to the difficulty of the theoretical treatment, but this is not treated in this work. Additionally, both problems, regular and irregular cases, share in common the problem of determining a concise manner of representing the similarity classes.

The paper's contribution is as follows. We study the 8T-LE partition applied to a regular tetrahedron. We prove that, for any initial regular tetrahedron  $R_0$ , the iterative 8T-LE partition of  $R_0$  produces a sequence of tetrahedra, where only two different similarity classes are generated. We used simple geometric arguments and a suitable tetrahedra representation to check the new classes generated. The cost of comparing two tetrahedra classes  $C_1$  and  $C_2$  implies only a comparison of two tetrahedra representations ( $C_1 = kC_2$ ), with  $k$  any positive real number. This process is computationally less expensive than the traditional definition involving orthogonal matrix computations, transposition, scaling, and translation in high-precision arithmetic.

As a consequence of the boundness of the number of similarity classes proven in the paper, the stability and regularity of the meshes obtained, as well as the minimum and maximum angle conditions are satisfied [12,13,22,23].

The outline of this paper is as follows. In Section 2, the sextuple representation for tetrahedra is introduced and discussed. Then, in Section 3, we study the classes generated by the 8T-LE of the regular tetrahedron. In Section 4, the evolution of each class is carried out. Finally, in Section 5, the strong stability of the meshes generated is proven.

## 2. Similarity Classes Based on an Efficient Tetrahedral Representation

Let  $T$  be an arbitrary non-degenerate tetrahedron with its six edge lengths  $a, b, c, d, e$ , and  $f$ , as in Figure 1. According to [24], a sextuple representation of  $T$  is given by six positive real numbers with the edge lengths  $T = (a,b,c,f,d,e)$  (see Figure 1a). The numbers  $a, b$ , and  $c$  are the lengths of the edges joining at a vertex  $T$ , and the numbers  $f, d$ , and  $e$  are the lengths of the corresponding edges opposite  $a, b$ , and  $c$ . So, an arbitrary tetrahedron  $T$  can be determined in  $4!$  ways by sextuples.

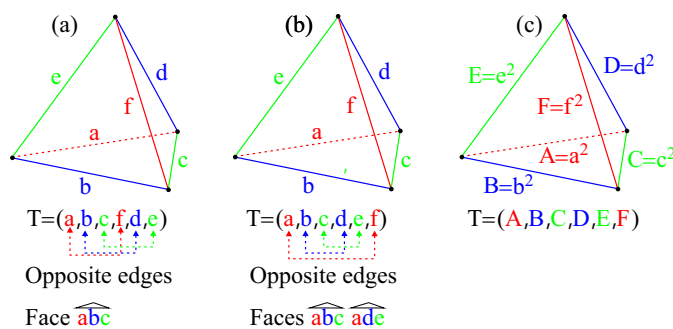
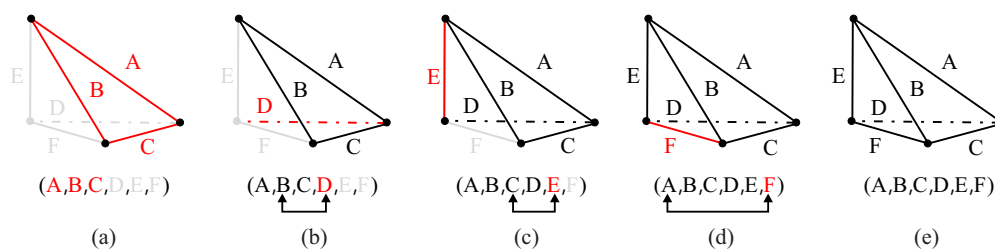


**Figure 1.** Two different sextuple representations for tetrahedron T. (a) Sextuple representation based on a vertex. (b,c) are the same sextuples focused on the relative position of the edges.

Among the sextuple representations based on the six edge lengths, we used the variant introduced in [25] and shown in Figure 1b. This sextuple representation cannot store tetrahedral coordinates. Instead, this sextuple is focused on keeping the relative positions of the edges. The key idea is to impose order on the edges within the sextuple, from left to right. Then, the ordering of edges lets us provide the relative positions of tetrahedron edges and faces, obtaining a unique way to represent the tetrahedron shape. Note also that the edge lengths are represented as squares of lengths. This is important to avoid roots when calculating the Euclidean distance. Then, the sextuple is in the form  $(a^2, b^2, c^2, d^2, e^2, f^2) = (A, B, C, D, E, F)$  (see Figure 1c). Also, square lengths allow us to calculate in a very easy way the four solid angles, the six dihedral angles, and the twelve planar angles around a vertex of a single tetrahedron, as well as the volume using the Cayley–Menger determinant, which involves square lengths [24]. Additionally, the shape quality measure  $\eta$  from Equation (2) is very easy to compute using square lengths.

As pointed out in [25], the sextuple used here guarantees that the pairs of opposite edges in the tetrahedron are always  $A–F$ ,  $B–D$ , and  $C–E$ , as seen in Figure 1b,c.

As we are studying the 8T-LE partition of tetrahedra, each time a subdivision is performed, eight new tetrahedron descendants appear and, then, eight sextuples need to be computed. Then, the normalization of the eight sextuples needs to be accomplished. Normalization is easily fixed if the first value in the sextuple is the longest edge and the second value the longest neighboring edge (see Figure 2).



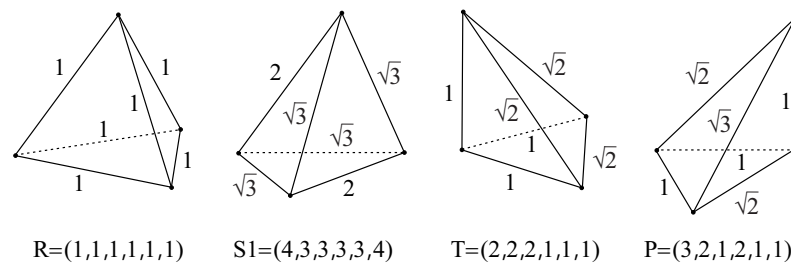
**Figure 2.** Building the normalized sextuple representation  $(A, B, C, D, E, F)$ . (a) The first three values in the sextuple. The three remaining values in the sextuple are shown in (b–d). (e) The normalized sextuple.

Figure 2 shows how the edges are picked up to set the normalized sextuple representation for a tetrahedron  $T = (A, B, C, D, E, F)$ . The longest edge  $A$  is always taken as the first value of the sextuple. The second value is  $B$ , the longest one from the four edges connected to  $A$ :  $B, C, D, E$ . Then,  $C$  closes the triangle  $\widehat{ABC}$ ; see Figure 2a.  $D$  is the edge opposite  $B$ ; see Figure 2b.  $E$  is the edge opposite  $C$ ; see Figure 2c. Finally,  $F$  is the last value, opposite  $A$ ; see Figure 2d. It can be seen that the normalized sextuple guarantees that  $A \geq B, C, D, E, F$  and  $B \geq C, D, E$ .

A very common situation in the longest-edge-based bisection is that the targeted tetrahedra to be bisected hold more than one longest edge. This is the case of the regular (equilateral) tetrahedra. To overcome this case, that is non-unique longest edges, the

normalized sextuple adopts the rule that places the highest possible values in the first position of the sextuple.

Figure 3 shows four examples of normalized sextuples for four well-known tetrahedra. From left to right are shown a regular tetrahedron with all its edges of length 1, a Somerville tetrahedron number of 1, a cube or trirectangular tetrahedron, and a path or right-type tetrahedron. Notice that, with this representation, the position and orientation of each tetrahedron are not taken into account, but only their geometric shape.



**Figure 3.** Four examples of normalized sextuple representations of tetrahedra.

**Definition 1.** A similarity class is a set of tetrahedra with the same geometric shape, regardless of their specific position, orientation, and scale. So, any two tetrahedra belonging to the same similarity class may be transformed to each other by an affine transformation.

The following definition relates this concept to our representation.

**Definition 2.** A similarity class is represented by  $k(A,B,C,D,E,F)$  in the normalized sextuple representation, for  $k \in \mathbb{R}^+$  being a scale factor.

Without loss of generality, from now on, we can omit the factor  $k$  and use brackets to represent a similarity class,  $[A,B,C,D,E,F]$ , and parenthesis to represent a single tetrahedron. In this manner,  $[A,B,C,D,E,F] = k(A,B,C,D,E,F), \forall k \in \mathbb{R}^+$ .

**Definition 3.** Given two tetrahedra,  $T_1$  and  $T_2$ , they belong to the same similarity class if  $T_1 = kT_2$ , with  $k \in \mathbb{R}^+$ .

The normalized sextuple representation is a suitable data structure for representing similarity classes of tetrahedra. Moreover, the cost of comparing two tetrahedra classes  $T_1$  and  $T_2$  given by their sextuple representations implies only a sextuple comparison ( $T_1 = kT_2$ ). This is computationally less expensive than other methods involving vertex-based representation, as in [19,26], that use matrix computations as determinants, transposition, scaling, and translation in high-precision arithmetic.

For brevity, we call a sextuple the normalized sextuple representation in the rest of the paper.

### 3. The 8T-LE Partition of a Regular Tetrahedron

In this section, we study the number of similarity classes produced by the 8T-LE partition applied to a regular tetrahedron.

**Definition 4.** In  $\mathbb{R}^n$ , a closed subset, say  $T$ , is called a  $k$ -simplex, where  $0 \leq k \leq n$ , if  $T$  is the convex linear hull of  $k + 1$  affinely independent vertices  $x^{(0)}, \dots, x^{(k)} \in \mathbb{R}^n$ :

$$T = [x^{(0)}, \dots, x^{(k)}] := \left\{ x = \sum_{j=0}^k \lambda_j x^{(j)} \mid \sum_{j=0}^k \lambda_j = 1; \lambda_j \in [0, 1], 0 \leq j \leq k \right\}.$$

When  $k = n$ ,  $T$  is named a simplex or element of  $\mathbb{R}^n$ . When  $k = 2, 3$  simplices are named triangles and tetrahedra.

**Definition 5.** The skeleton of an  $n$ -simplicial mesh,  $\tau$ , is the set  $skt(\tau) = \{f : f \text{ is an } (n - 1)\text{-face of any } T_i, \text{ with } T_i \in \tau\}$ . The skeleton is also called an  $(n - 1)$ -skeleton.

For example, the skeleton of a tetrahedral mesh is the set of the faces of the tetrahedra, and the skeleton of a triangular mesh is the set of the edges. The skeleton can be applied recursively:

$$1\text{-skt}(\tau) \subset 2\text{-skt}(\tau) \subset \dots \subset (n - 1)\text{-skt}(\tau).$$

Plaza and Carey introduced and studied the 8T-LE partition [8]. See also [16,18] for different features of this partition.

**Definition 6.** The four-triangle longest-edge partition (4T-LE) of triangle  $t_1$  works as follows: the first triangle  $t_1$  is divided by its longest edge (see Figure 4a), producing new subtriangles  $t'$  and  $t''$ . Then, it follows the edge bisection of  $t'$  and  $t''$  by the remaining edges of  $t_1$ ; see Figure 4b. The 4T-LE partition generates two triangles  $t_1$  similar to the original one and two triangles  $t_2$  similar to each other.

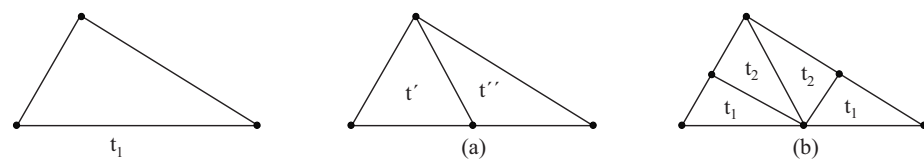


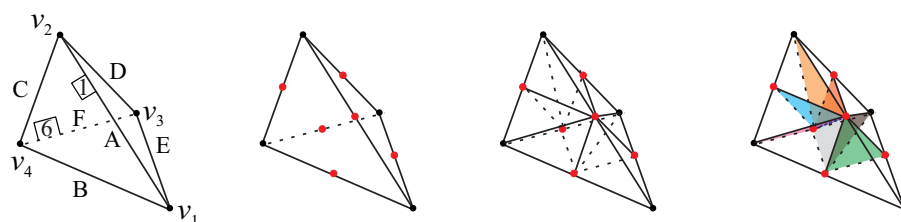
Figure 4. (a) LE bisection of  $t_1$ . (b) Triangle  $t_1$  after applying the 4T-LE.

**Definition 7.** The eight-tetrahedron longest-edge partition (8T-LE) of a tetrahedron  $T$  works as follows: First, the 4T-LE partition is applied to the skeleton (see Figures 4b and 5c). Then, the interior of  $T$  is divided according to the division of triangular faces (see Figure 5d). As a result, eight subtetrahedra are obtained.

It is important to remark that, before applying the 8T-LE partition to any tetrahedron, the tetrahedron has to be previously classified into one of three types taking into account the relative positions of the longest edges of the faces [8].

**Definition 8.** For any tetrahedron  $T$ , the primary edges are the longest edges of two faces sharing them. These faces are called primary faces of  $T$ . Notice that, in any tetrahedron, it may be one or two primary edges. If there is a unique primary edge, the longest edge  $T$ , then the two remaining faces of  $T$  are called secondary faces. Furthermore, the secondary edges of  $T$  are the longest edges of the secondary faces of  $T$ . Tertiary edges are the remaining edges of  $T$ .

Figure 5 shows an example of the 8T-LE partition applied to a tetrahedron with vertices  $v_1, v_2, v_3$ , and  $v_4$ , where the primary edge is  $A$ , and the edges  $F$  and  $B$  are the secondary edges.



(a) Initial tetrahedron (b) 1-Skeleton Subdivision (c) 2-Skeleton Subdivision (d) Interior Subdivision

**Figure 5.** The 8T-LE partition of a tetrahedron  $T = (A,B,C,D,E,F)$ . (a) shows a targeted tetrahedron to be subdivided. The edges are marked in (b). In (c), the triangular faces are subdivided. Eight subtetrahedra are obtained in (d).

Figure 6 shows the longest edge of four tetrahedra and the opposite edge to the longest one labeled respectively with 1 and 6. Edge number 1 is also a primary edge and, so, the longest edge of the two faces sharing it, marked in red in Figure 6. The other two faces have other longest edges, marked in blue in Figure 6 (secondary edges). If edge number 6 is a tertiary edge, it is not the longest edge of the faces sharing it, and the tetrahedron is Type 1 (see Figure 6a). If edge number 6 is also a primary edge, the longest edge of the two faces sharing it, the tetrahedron is Type 2 (see Figure 6b). In another case, that is edge number 6 is a secondary edge, the longest edge of one of the faces sharing it, and the tetrahedron is Type 3 (see Figure 6c).

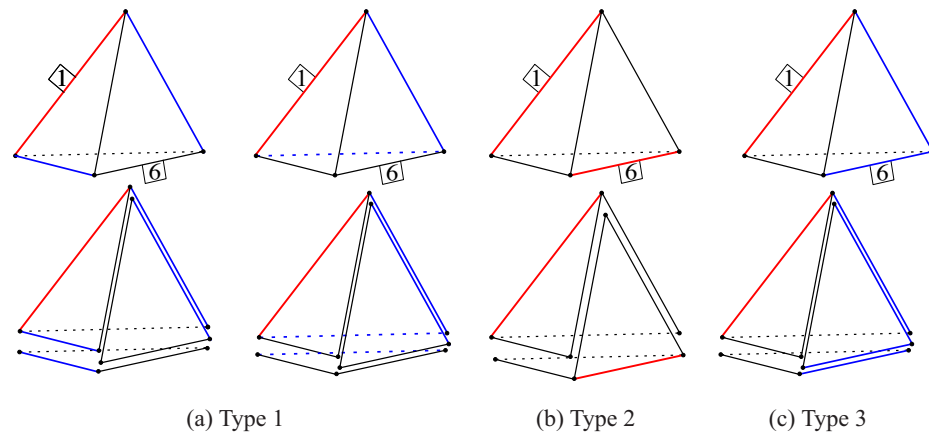


**Figure 6.** Classification of tetrahedra. The primary edges are in red; the secondary edges are in blue; the tertiary edges are in black.

The classification of a single tetrahedron is as follows [8]:

**Procedure classification**

```
% Input variable: tetrahedron T;
% Output variables: tetrahedron type;
If edge 6 is a tertiary edge, then:
    T is Type 1 (see Figure 6a);
Else edge 6 is a primary edge, then:
    T is Type 2 (see Figure 6b);
Else edge 6 is a secondary edge, then:
    T is Type 3 (see Figure 6c);
End if.
```

The 8T-LE partition of a tetrahedron T can be described as follows [27]:

**The 8T-LE partition;**

```
% Input variable: tetrahedron T;
% Output variables: eight new subtetrahedra;
1. Procedure classification of T;
2. 4T-LE applied to the skeleton of T;
3. Division of the interior of T.
```

Since a regular tetrahedron has six edges of an equal length, the main challenge is how to classify it according to the procedure classification. Theoretically, the regular tetrahedron can be any of the three types. Before choosing one of the three types, it is important to take into account that the 8T-LE partition of a single tetrahedron T can also be obtained by three steps of bisection as follows:

1. Bisection of  $T$  by the longest edge (primary edge) generating subtetrahedra  $T_1$  and  $T_2$ .
2. Bisection of  $T_1$  and  $T_2$  by the primary or secondary edge  $T_1$  and  $T_2$ , generating subtetrahedra  $T_{11}, T_{12}, T_{21}$ , and  $T_{22}$ .
3. Bisection of the tetrahedra obtained in Step 2 by the tertiary edges, producing eight subtetrahedra,  $T_{111}, T_{112}, T_{121}, T_{122}, T_{211}, T_{212}, T_{221}$ , and  $T_{222}$ .

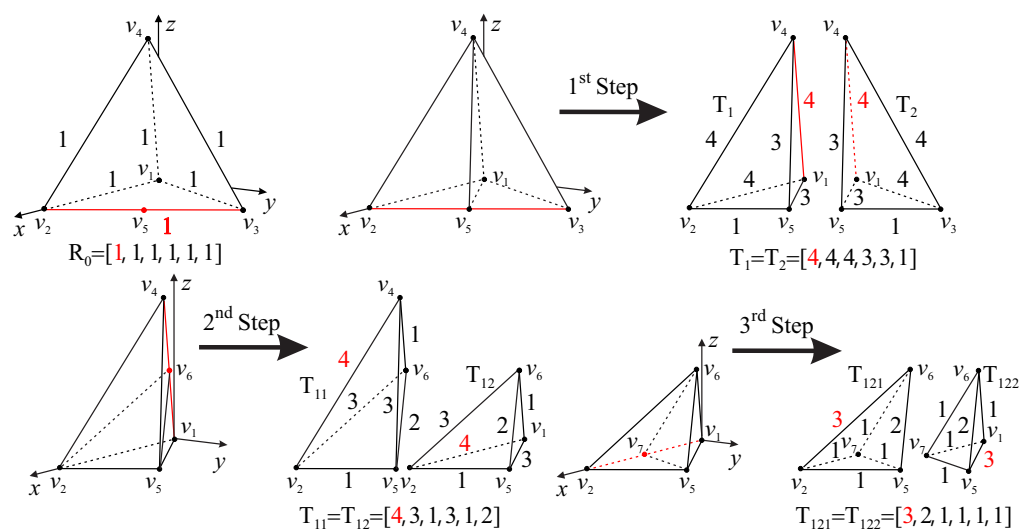
Therefore, this partition can also be seen as the longest-edge bisection [11] applied three times to a single tetrahedron  $T$ . In some cases, both partitions are equivalent [16]. So, the idea is to choose the type that makes both partitions equivalent, since the LEB of a regular tetrahedron produces a finite number of similarity classes [19].

Figure 7 shows the first three steps of the LEB applied to  $R_0$ . For the first step, it does not matter which of the edges is chosen, because all of them are of equal length. For instance, we take the first value in the sextuple  $R_0 = [1, 1, 1, 1, 1, 1]$ , which is marked in red. Because of the symmetry of  $R_0$ , the first two subtetrahedra are similar to each other:  $T_1 = T_2 = [4, 4, 4, 3, 3, 1]$ .

For the second step, we have three longest edges of equal length. It is clear that, if we choose as the longest edge the edge marked in red in the sextuple, the generated subtetrahedra are similar to one another at this level,  $T_{11} = T_{12} = T_{21} = T_{22} = [4, 3, 1, 3, 1, 2]$ . Finally, in the third step, all generated subtetrahedra are similar to each other with normalized sextuple  $[3, 2, 1, 1, 1, 1]$ .

The 8T-LE partition will be equivalent to the LEB, if and only if the regular tetrahedron is classified as Type 2. This classification of the regular tetrahedron is coherent since, when an edge of  $R_0$  is chosen as the longest one (primary edge), this edge is also the longest of the two faces sharing it. So, the only way for another edge to be a primary edge and, therefore, the longest one of the remaining two faces sharing it is to be opposite the first one, that is  $R_0 = [1, 1, 1, 1, 1, 1]$ .

It is also interesting to highlight that, although Adler did not give a rigorous definition of “nearly equilateral” tetrahedra [21], these tetrahedra should hold that the longest edge and the second-longest edge both have to be opposite each other, to ensure his conjecture. So, all nearly equilateral tetrahedra are also classified as Type 2.



**Figure 7.** The first three steps of the LEB are applied to  $R_0$ . In the first step, two subtetrahedra similar to each other are generated. Those subtetrahedra have three longest edges of equal length, and for the second step, they are subdivided by the first value of the sextuple (in red). The third step shows the subtetrahedra produced.

**Theorem 1.** Let  $R_0$  be a regular tetrahedron. Then, after applying three steps of the 8T-LE partition to  $R_0$ , two different similarity classes appear.

**Proof.** Our proof uses simple geometrical arguments together with Definition 3. Figure 8 shows the similarity classes generated when the 8T-LE partition is applied to a regular tetrahedron with vertices  $v_1 = (0,0,0)$ ,  $v_2 = (1,0,0)$ ,  $v_3 = (\frac{1}{2}, \frac{\sqrt{3}}{2}, 0)$ , and  $v_4 = (\frac{1}{2}, \frac{1}{2\sqrt{3}}, \sqrt{\frac{2}{3}})$ . The eight generated subtetrahedra regrouped by pairs are similar to each other, but not to the original one (see Figure 8). In this step, a new class is generated. Figure 9 shows the 8T-LE partition applied to the new class  $R_1 = [3, 2, 1, 1, 1, 1]$ , generated in the first step. In this case, only a new class is generated  $R_2 = [2, 1, 1, 1, 1, 1]$ .

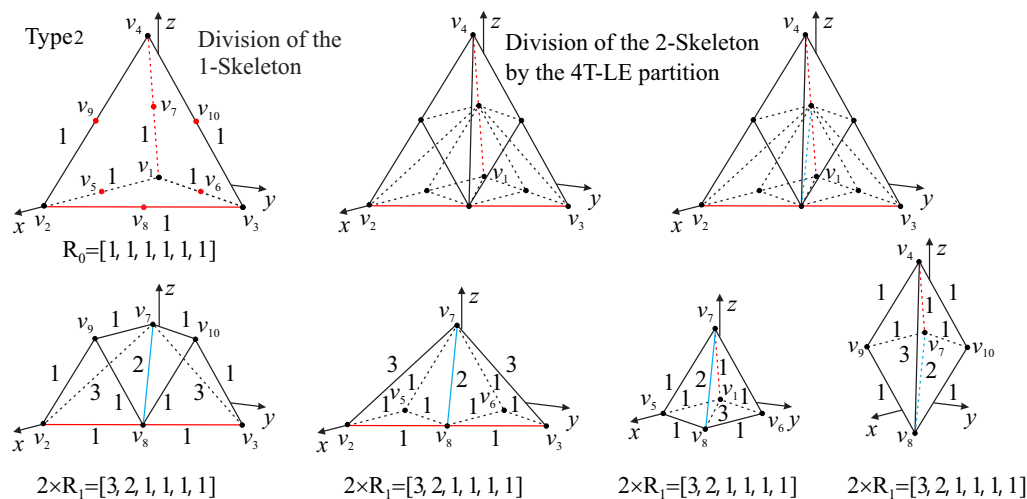


Figure 8. The similarity classes generated by the 8T-LE partition of a regular tetrahedron.

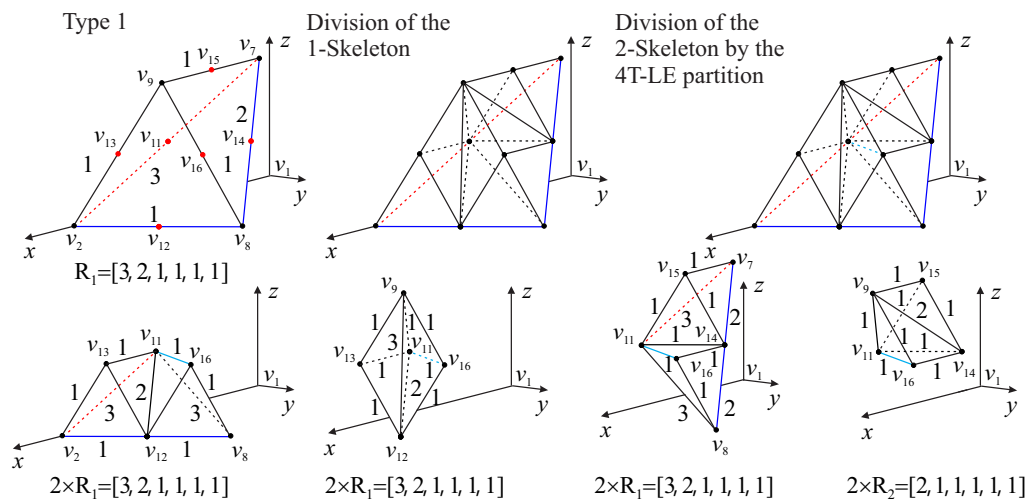


Figure 9. The similarity classes generated by the 8T-LE partition applied to  $R_1$ .

Finally, Figure 10 shows that no new different similarity classes appear when the 8T-LE partition is applied to  $R_2$ .

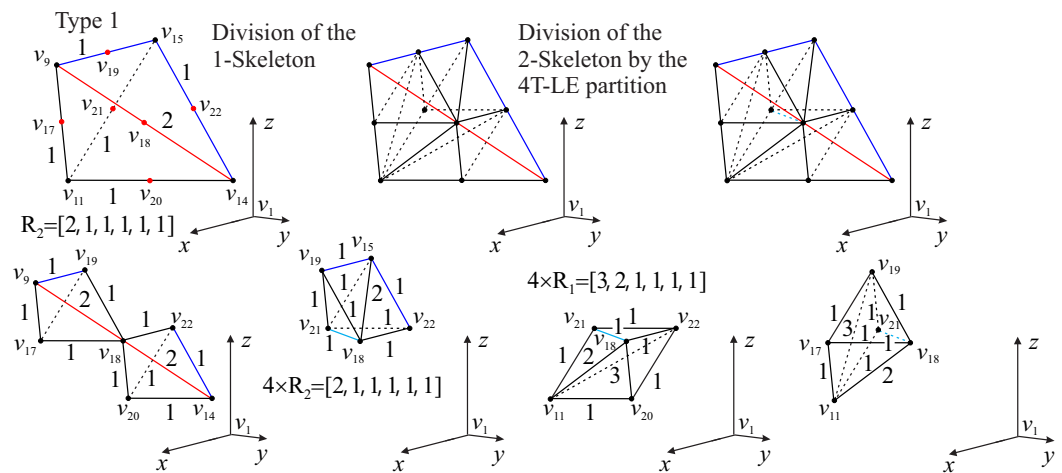


Figure 10. The similarity classes generated by the 8T-LE partition applied to  $R_2$ . □

**Corollary 1.** The 8T-LE partition of a regular tetrahedron  $R_0$  does not degenerate.

Figure 11 shows the binary tree of the similarity classes generated by the 8T-LE partition applied to  $R_0$ .

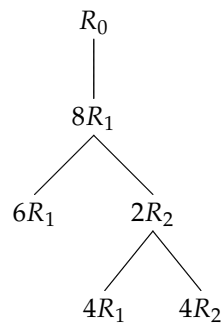


Figure 11. A binary tree of the similarity classes of a regular tetrahedron.

**4. Evolution of Each Similarity Class**

Let  $R_i^{(n)}$  denote the number of tetrahedra of class  $R_i$  for  $i = 0, 1, 2$ , after  $n$  iterative applications of the 8T-LE partition to an initial regular tetrahedron  $R_0 = R_0^{(0)}$ . Notice that, since  $R_0^{(0)} = 1$  and  $\forall n \geq 1, R_0^{(n)} = 0$ , we considered  $n = 1$  as our initial step. So, it can be written as  $k = n - 1$ . The recurrence relations related to the 8T-LE partition applied to an initial regular tetrahedron  $R_0$ , where the initial conditions are  $R_1^{(0)} = 8$  and  $R_2^{(0)} = 0$ , follow:

$$\begin{cases} R_1^{(k)} = 6R_1^{(k-1)} + 4R_2^{(k-1)} \\ R_2^{(k)} = 2R_1^{(k-1)} + 4R_2^{(k-1)} \end{cases} \text{ for } k \geq 1. \tag{1}$$

**Theorem 2.** Let  $R_0$  be a regular tetrahedron. Then, after  $k$  applications of the 8T-LE partition, then

$$R_1^{(k)} = \frac{2^{3k+4} + 2^{k+3}}{3}, \quad R_2^{(k)} = \frac{2^{3k+3} - 2^{k+3}}{3}.$$

**Proof.** Equation (1) may be written in matrix form as

$$\begin{pmatrix} 6 & 4 \\ 2 & 4 \end{pmatrix} \times \begin{pmatrix} R_1^{(k-1)} \\ R_2^{(k-1)} \end{pmatrix} = \begin{pmatrix} R_1^{(k)} \\ R_2^{(k)} \end{pmatrix}$$

Since

$$\begin{pmatrix} 6 & 4 \\ 2 & 4 \end{pmatrix} = \begin{pmatrix} -1 & 2 \\ 1 & 1 \end{pmatrix} \cdot \begin{pmatrix} 2 & 0 \\ 0 & 2^3 \end{pmatrix} \cdot \begin{pmatrix} -\frac{1}{3} & \frac{2}{3} \\ \frac{1}{3} & \frac{1}{3} \end{pmatrix},$$

then

$$\begin{pmatrix} 6 & 4 \\ 2 & 4 \end{pmatrix}^k = \begin{pmatrix} -1 & 2 \\ 1 & 1 \end{pmatrix} \cdot \begin{pmatrix} 2^k & 0 \\ 0 & 2^{3k} \end{pmatrix} \cdot \begin{pmatrix} -\frac{1}{3} & \frac{2}{3} \\ \frac{1}{3} & \frac{1}{3} \end{pmatrix},$$

from which and taking into account the initial conditions  $R_1^{(0)} = 8$  and  $R_2^{(0)} = 0$ , it follows that

$$\begin{pmatrix} R_1^{(k)} \\ R_2^{(k)} \end{pmatrix} = \begin{pmatrix} 6 & 4 \\ 2 & 4 \end{pmatrix}^k \cdot \begin{pmatrix} 8 \\ 0 \end{pmatrix} = \begin{pmatrix} -1 & 2 \\ 1 & 1 \end{pmatrix} \cdot \begin{pmatrix} 2^k & 0 \\ 0 & 2^{3k} \end{pmatrix} \cdot \begin{pmatrix} -\frac{1}{3} & \frac{2}{3} \\ \frac{1}{3} & \frac{1}{3} \end{pmatrix} \cdot \begin{pmatrix} 8 \\ 0 \end{pmatrix}$$

and, after some algebra, we obtain the result.  $\square$

Figure 12 shows the variation of the volume of the  $R_0, R_1,$  and  $R_2$  classes (in percentage) as the number of the 8T-LE steps of refinement grows. The regular tetrahedron class is no longer generated from the first step, and only two new classes appear in each refinement step. Then, the 8T-LE iterative application of a regular tetrahedron is optimal in the sense that it produces the minimum number of similarity classes. One can compare, for example, with the case of the longest-edge bisection, for which it was shown in [19] that it converges into eight similarity classes.

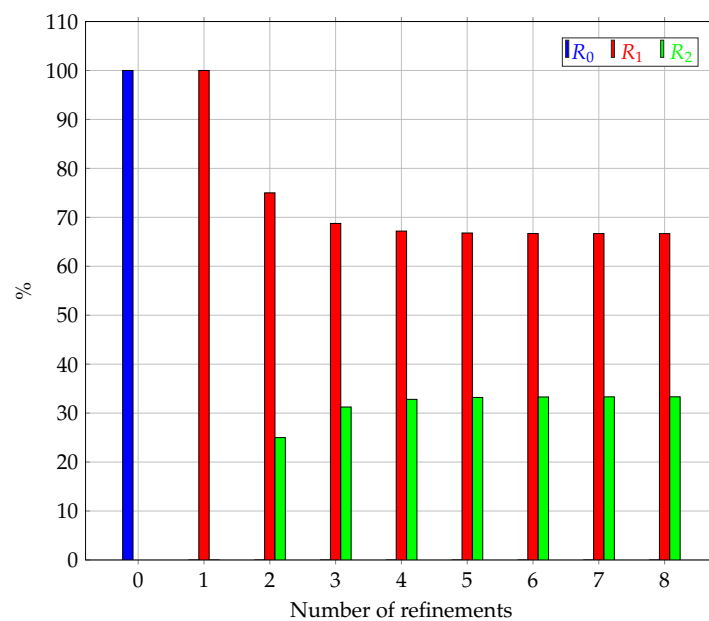


**Figure 12.** Percentage of volume of the  $R_0, R_1,$  and  $R_2$  classes as the number of 8T-LE steps of refinement grows.

Now, we calculate the limit when  $k$  tends to infinity of these expressions,  $\lim_{k \rightarrow \infty} \frac{R_1^{(k)}}{R_1^{(k)} + R_2^{(k)}}$  and  $\lim_{k \rightarrow \infty} \frac{R_2^{(k)}}{R_1^{(k)} + R_2^{(k)}}$ . For the first one,

$$\lim_{k \rightarrow \infty} \frac{R_1^{(k)}}{R_1^{(k)} + R_2^{(k)}} = \lim_{k \rightarrow \infty} \frac{\frac{2^{3k+4} + 2^{k+3}}{3}}{\frac{2^{3k+4} + 2^{k+3}}{3} + \frac{2^{3k+3} - 2^{k+3}}{3}} = \frac{2}{3}.$$

Hence, the limit for the second expression is equal to  $\frac{1}{3}$ .

**Corollary 2.** *Let  $R_0$  be a regular tetrahedron and  $R_1$  and  $R_2$  the new similarity classes. Then, the volumes covered by classes  $R_1$  and  $R_2$  tend, respectively, to  $\frac{2}{3}$  and  $\frac{1}{3}$  of the initial volume, as the number of global refinements  $k$  tends to infinity.*

### 5. Stability and Non-Degeneracy of Tetrahedral Meshes Generated

Let  $\tau^0 = \{R_0\}$  be an initial mesh with a unique regular tetrahedron  $R_0$ . By iteratively applying the 8T-LE partition, a sequence of tetrahedral meshes  $\tau^0, \tau^1, \tau^2 \dots$  is obtained.

We used the notation  $\tau^n$  for the  $n$ -times uniformly refined tetrahedral meshes.

**Definition 9.** *For a shape quality measure  $\zeta$ , a partitioning method is said to be stable [28] if, for any initial mesh  $\tau^0$ , the shape quality remains bounded away from zero for all tetrahedra, which means there is a constant  $c > 0$  such that*

$$\zeta_{\min}(\tau^n) := \min_{T \in \tau^n} \zeta(T) \geq c \quad \forall n$$

independent of  $n$ .

**Definition 10.** *For a shape quality measure  $\zeta$ , a partitioning method is said to be strongly stable if there is a constant  $c > 0$  (independent of the initial mesh  $\tau^0$  and the step of refinement  $n$  [28]) such that*

$$\zeta_{\min}(\tau^n) \geq c \zeta_{\min}(\tau^0).$$

Obviously, strong stability implies stability, but the definition of strong stability depends on the shape quality measure chosen; but, stability does not [28].

For a single tetrahedron  $T$ , we used here the shape quality measure  $\eta$  introduced by Liu and Joe [14], defined by

$$\eta(T) = \frac{12(3V)^{2/3}}{\sum_{i=1}^6 l_i^2}, \tag{2}$$

where  $V$  is the volume and  $l_i$  are the edge lengths of  $T$ .

For this standard shape measure ( $\eta$ ) and for any tetrahedron  $R_i^n$  in  $\tau^n$ , there is a positive constant  $c$  independent of  $n$  and  $i$  such that

$$\eta(R_i^n) \geq c \eta(R_0). \tag{3}$$

For a triangulation  $\tau^n$ , a quality measure is given by  $\eta(\tau^n) = \min\{\eta(R_i^n)\}$  for all  $R_i^n \in \tau^n$ . Therefore, the value

$$c_n = \frac{\eta(\tau^n)}{\eta(\tau^0)} \tag{4}$$

is calculated. Since only two new similarity classes are generated and according to Equation (2),  $\eta(R_1) = \frac{2}{3}$  and  $\eta(R_2) = \frac{6}{7}$ , so  $c = \frac{2}{3}$ . By Definition 10, the 8T-LE partition is strongly stable with respect to  $\eta$  with  $c = \frac{2}{3}$ .

## 6. Conclusions

The 8T-LE partition applied to a regular tetrahedron was carried out. It was proven with an efficient tetrahedral representation, called the normalized sextuple, that this partition only generates two different similarity classes. All generated tetrahedra are  $R_1$  or  $R_2$ . Note that, in the numerical computations, we desired that the number of similarity classes be not only finite, but even as small as possible [29]. This plays a very significant role in saving CPU time, and in some cases, superconvergence phenomena can be achieved.

Additionally, for the shape quality measure  $\eta$ , a positive non-degeneracy constant was obtained,  $c = \frac{2}{3}$ , which proves the strong stability for the generated meshes. Let  $\tau^0, \tau^1, \tau^2, \dots, \tau^n, \dots$  be the sequence of tetrahedral meshes obtained by the iterative application of the 8T-LE partition to an initial regular tetrahedron  $R_0$  and its successors. For any tetrahedron  $R_i^n \in \tau^n$ ,  $\eta(R_i^n) \geq \frac{2}{3}\eta(R_0)$  and constant  $\frac{2}{3}$  is independent of  $i$  and  $n$ .

Therefore, the regularity and non-degeneracy of the meshes, as well as the minimum and maximum angle condition follow straightforwardly.

As future work, we can study the octasection method applied to the regular tetrahedron, which it is not based on the bisection method.

**Author Contributions:** Methodology, M.A.P. and Á.P.; Software, J.P.S.; Investigation, M.A.P. and Á.P.; Writing—review & editing, M.A.P. and Á.P.; Visualization, J.P.S.; Supervision, M.A.P. All authors have read and agreed to the published version of the manuscript.

**Funding:** This research was funded by “Fundación Parque Científico y Tecnológico de la ULPGC” grant reference “F2021/05 FEI Innovación y Transferencia empresarial en material científico tecnológica en la rama Geoinformática y datos”.

**Conflicts of Interest:** The authors declare no conflict of interest.

## References

- Zienkiewicz, O.C.; Liu, Y.C.; Huang, G.C. Error estimation and adaptivity in flow formulation for forming problems. *Int. J. Num. Meth. Eng.* **1988**, *25*, 23–42. [[CrossRef](#)]
- Zienkiewicz, O.C.; Zhu, J.Z.; Gong, N.G. Effective and partial h-p version adaptive analysis procedures for the finite element method. *Int. J. Num. Meth. Eng.* **1989**, *28*, 879–891. [[CrossRef](#)]
- Bey, J. Tetrahedral grid refinement. *Computing* **1995**, *55*, 355–378. [[CrossRef](#)]
- Liu, A.; Joe, B. Quality local refinement of tetrahedral meshes based on 8-subtetrahedron subdivision. *Math. Comp.* **1996**, *65*, 1183–1200. [[CrossRef](#)]
- Zhang, S. Successive subdivisions of tetrahedra and multigrid methods on tetrahedral meshes. *Houston J. Math.* **1995**, *21*, 541–556.
- Arnold, D.N.; Mukherjee, A.; Pouly, L. Locally adapted tetrahedral meshes using bisection. *SIAM J. Sci. Comp.* **2000**, *22*, 431–448. [[CrossRef](#)]
- Bänsch, E. Local mesh refinement in 2 and 3 dimensions. *IMPACT Comp. Sci. Engrg.* **1991**, *3*, 181–191. [[CrossRef](#)]
- Plaza, Á.; Carey, G.F. Local refinement of simplicial grids based on the skeleton. *Appl. Num. Math.* **2000**, *32*, 195–218. [[CrossRef](#)]
- Liu, A.; Joe, B. Quality of local refinement of tetrahedral meshes based on bisection. *SIAM J. Sci. Comp.* **1995**, *16*, 1269–1291. [[CrossRef](#)]
- Maubach, J.M. Local bisection refinement for  $n$ -simplicial grids generated by reflection. *SIAM J. Sci. Comp.* **1995**, *16*, 210–227. [[CrossRef](#)]
- Rivara, M.C.; Levin, C. A 3-D refinement algorithm suitable for adaptive and multi-grid techniques. *J. Comp. App. Math.* **1992**, *8*, 281–290.
- Babuška, I.; Aziz, A.K. On the angel condition in the finite element method. *SIAM J. Num. Anal.* **1976**, *13*, 214–226. [[CrossRef](#)]
- Ženišek, A. The maximum angle condition in the finite element method for monotone problems with applications in magnetostatics. *Num. Math.* **1995**, *71*, 399–417. [[CrossRef](#)]
- Liu, A.; Joe, B. On the shape of tetrahedra from bisection. *Math. Comp.* **1994**, *63*, 141–154. [[CrossRef](#)]
- Kossaczky, I. A recursive approach to local mesh refinement in two and three dimensions. *J. Comp. App. Math.* **1994**, *55*, 275–288. [[CrossRef](#)]
- Padrón, M.A.; Suárez, J.P.; Plaza, Á. A comparative study between some bisection based partitions in 3D. *Appl. Num. Math.* **2005**, *55*, 357–367. [[CrossRef](#)]
- Rivara, M.C. Algorithms for refining triangular grids suitable for adaptive and multigrid techniques. *Int. J. Num. Meth. Eng.* **1984**, *20*, 745–756. [[CrossRef](#)]

18. Plaza, Á.; Padrón, M.A.; Suárez, J.P. Non-degeneracy study of the 8-tetrahedra longest-edge partition. *Appl. Num. Math.* **2005**, *55*, 458–472. [[CrossRef](#)]
19. Aparicio, G.; Casado, L.G.; Hendrix, E.M.T.; G.-Tóth, B.; García, I. On the minimum number of simplex shapes in longest edge bisection refinement of a regular  $n$ -simplex. *Informatica* **2015**, *26*, 17–32. [[CrossRef](#)]
20. Salmerón, J.M.G.; Aparicio, G.; Casado, L.G.; García, I.; Hendrix, E.M.T.; G.-Tóth, B. Generating a smallest binary tree by proper selection of the longest edges to bisect in a unit simplex refinement. *J. Comb. Optim.* **2015**, *33*, 389–402. [[CrossRef](#)]
21. Adler, A. On the bisection method for triangles. *Math. Comp.* **1983**, *40*, 571–574. [[CrossRef](#)]
22. Hannukainen, A.; Korotov, S.; Křížek, M. The maximum angle condition is not necessary for convergence of the finite element method. *Num. Math.* **2011**, *120*, 79–88. [[CrossRef](#)]
23. Zlamal, M. On the finite element method. *Num. Math.* **1968**, *12*, 394–409. [[CrossRef](#)]
24. Wirth, K.; Dreiding, A. Edge length determining tetrahedrons. *Elem. Math.* **2009**, *64*, 160–170. [[CrossRef](#)] [[PubMed](#)]
25. Suárez, J.P.; Trujillo, A.; Moreno, T. Computing the exact number of similarity classes in the longest edge bisection of tetrahedra. *Mathematics* **2021**, *9*, 1447. [[CrossRef](#)]
26. Hannukainen, A.; Korotov, S.; Křížek, M. On numerical regularity of the face-to-face longest-edge bisection algorithm for tetrahedral partitions. *Sci. Comput. Program.* **2014**, *90*, 34–41. [[CrossRef](#)]
27. Padrón, M.A.; Plaza, Á. The 8T-LE partition applied to the obtuse triangulations of the 3D-cube. *Math. Comp. Simu.* **2020**, *176*, 254–265. [[CrossRef](#)]
28. Kröger, T.; Preusser, T. Stability of the 8-tetrahedra shortest-interior-edge partitioning method. *Num. Math.* **2008**, *109*, 435–457. [[CrossRef](#)]
29. Křížek, M. Superconvergence phenomena on three-dimensional elasticity. *Int. J. Num. Anal. Model.* **2005**, *2*, 43–56.

**Disclaimer/Publisher's Note:** The statements, opinions and data contained in all publications are solely those of the individual author(s) and contributor(s) and not of MDPI and/or the editor(s). MDPI and/or the editor(s) disclaim responsibility for any injury to people or property resulting from any ideas, methods, instructions or products referred to in the content.